



Kristopher L. Kuhlman¹, Forest T. Good^{1,4}, Melissa M. Mills¹, Matthew J. Paul¹, Jason E. Heath², Tara LaForce³, Brittney D. Seaburn¹
Sandia National Laboratories: ¹Nuclear Waste Disposal Research & Analysis, ²Geomechanics, ³Applied Systems Analysis & Research; ⁴New Mexico Institute of Mining and Technology

1. Background and Zeolitic Test Results

We need to estimate two-phase flow properties for vadose zone rocks for site characterization efforts, especially for gas transport in the vadose zone from an underground explosion (Heath et al., 2021). Kuhlman et al. (2022b) adapted an approach proposed by Peters et al. (1987) to estimate properties from transient imbibition experiments. It traded a more complex test interpretation (i.e., numerical model and parameter estimation) for simpler test execution in the laboratory (i.e., a single transient imbibition test). To constrain the model, the test monitors uptake of water by a sample while tracking the progress of the wetting front height.

Previous work (Kuhlman et al., 2022b) monitored the wetting front progress with images. We monitored the change in temperature in the core using resistance temperature detectors (RTDs) attached to the sample with rubber bands (Fig 1).

The imbibition test measured the mass loss from a constant-head Mariotte bottle (Fig 2), while monitoring the temperature at locations along the sides of the sample. Electrical resistance across the sample itself was also measured.

For zeolitic tuff cores (up to 60% zeolite minerals like clinoptilolite), there was a clear separation observed between the arrival of the visible wetting front and the arrival of the thermal front. The wetting front height was estimated from images and from the mass of water imbibed data (Fig 3).



Fig 1. Zeolitic tuff core sample (left) with RTDs attached (right) used in imbibition experiments.

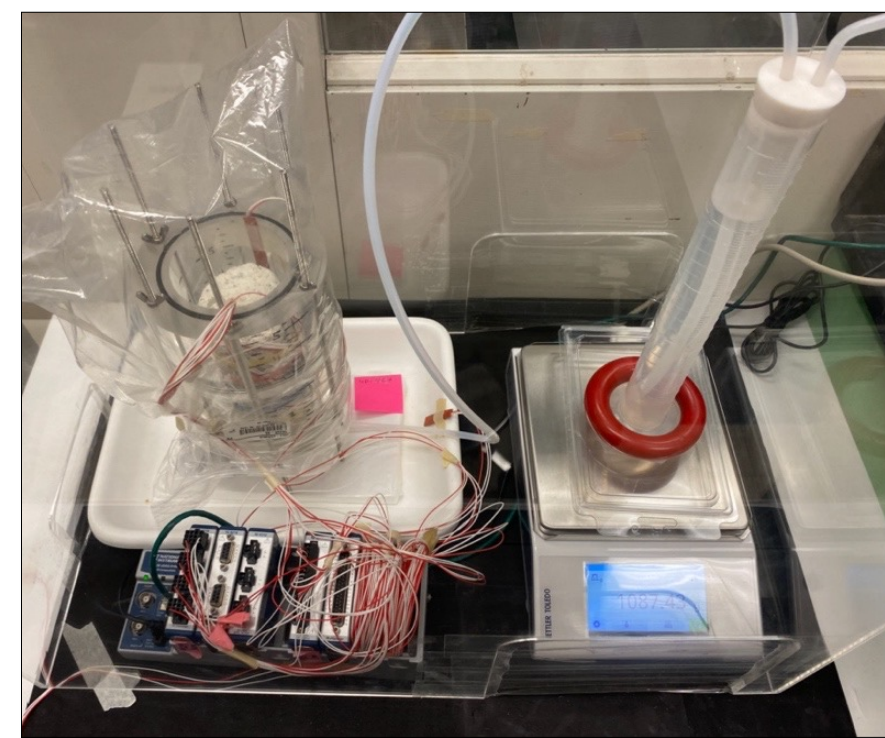


Fig 2. Sandia thermal imbibition test setup. Sample holder (upper left), Mariotte bottle on balance (right), and data acquisition (lower left); Kuhlman et al. (2022)

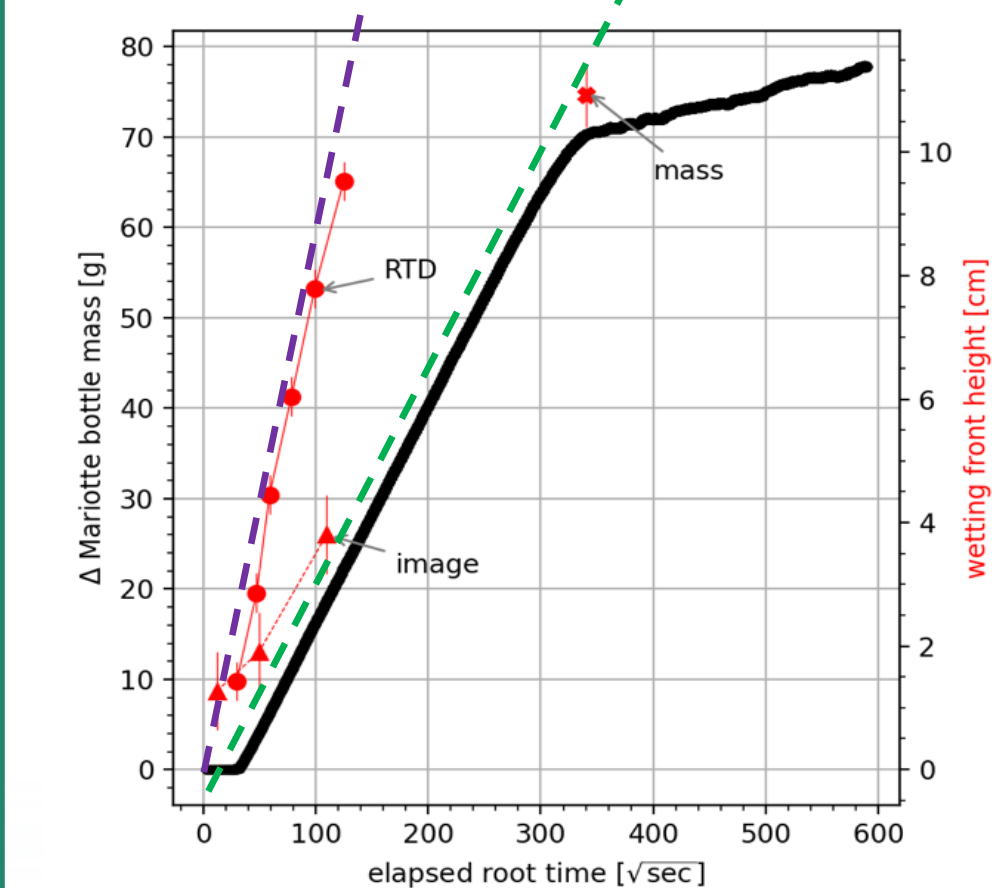


Fig 3. Mass imbibed (black) wetting front observed visually (▲) and via RTDs (●) vs. root time for zeolitic tuff core. Green line is $7.46 \times 10^{-5} \text{ m}/\sqrt{\text{s}}$ slope

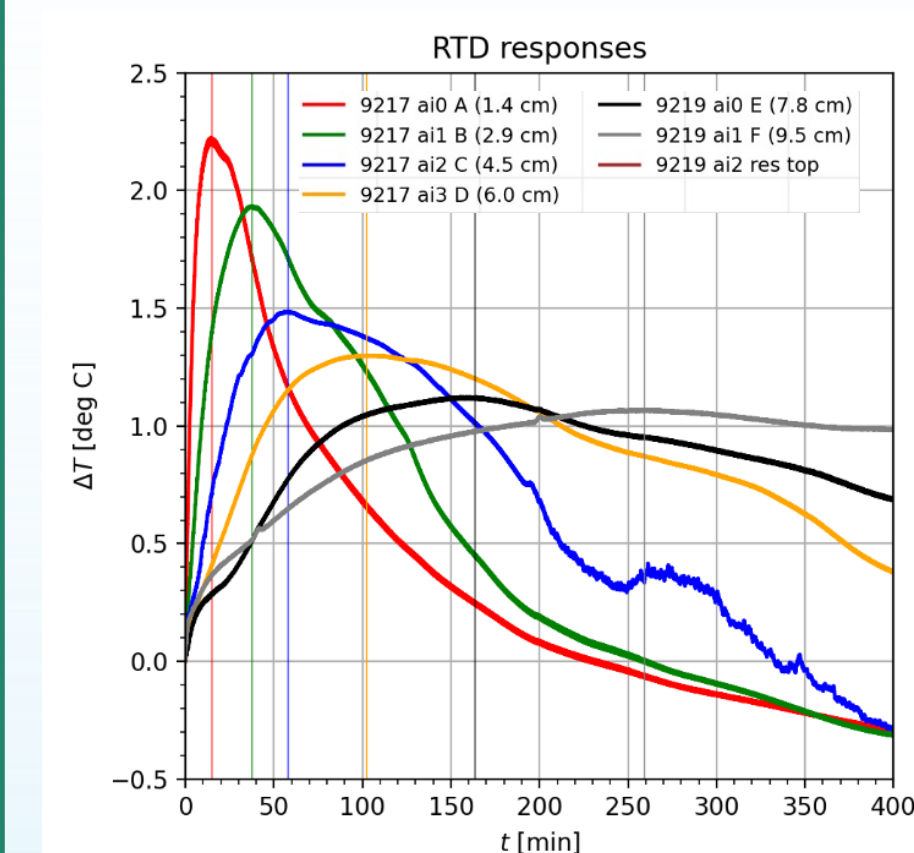


Fig 4. Temperature change in zeolitic core (Good et al., 2023)

The data from zeolitic core indicated two clear speeds of fronts moving up the sample (slopes of dashed lines in Fig 3). Faster transport was associated with first arrival of a temperature peak (purple line, 4.3 hours to top RTD), while slower transport was associated with the arrival of liquid water at a point in the sample (green line, 25 hours to top RTD).

The time to peak temperature at each location (Fig 4) are each plotted with position on Fig 3 as red circles (Kuhlman et al., 2022a).

2. Physical Processes

Spontaneous imbibition of water into porous media is an exothermic process. This can be caused by two processes: adsorption of water vapor or adhesion of liquid water (i.e., immersion). These are like phase-change processes (Fig 5).

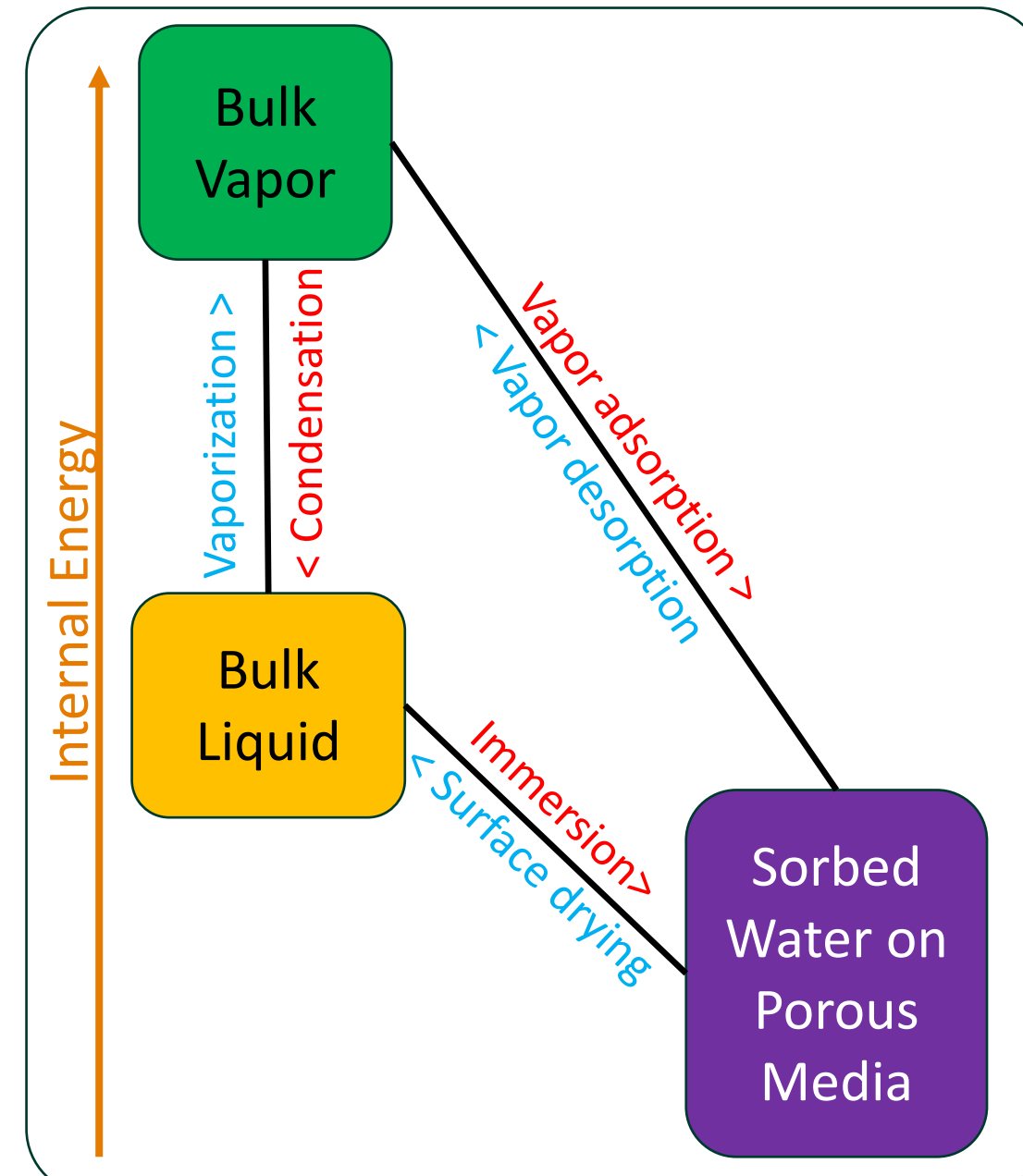


Fig 5. Phase changes in a microporous medium. Exothermic processes are red, endothermic processes are blue.

Zeolites are common alteration products where weathering of volcanic glass occurs. Zeolites have cage-like molecular structures which can trap some molecules.

Gas molecules that adsorb onto a wetting surface are at a lower chemical potential than the bulk state, releasing thermal energy. The cage-like structure of zeolites may present an even lower chemical potential than planar surfaces, resulting in a comparatively large release of energy for vapor adsorption (Żołądek-Nowak et al., 2012).

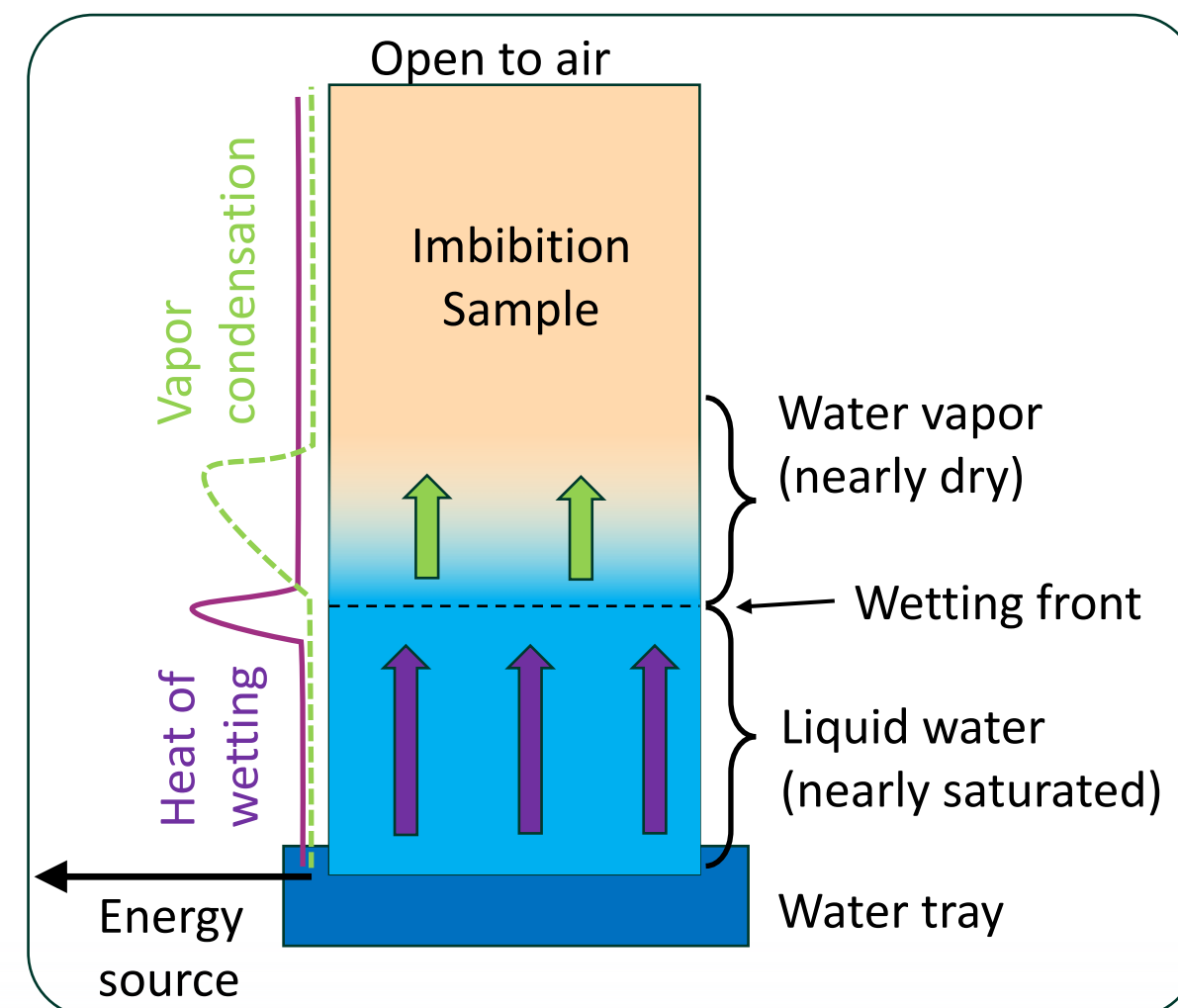


Fig 6. Diagram (left) showing relative locations where heat of wetting and vapor condensation occur.

Heat of wetting releases sensible heat at the wetting front (Murali et al., 2020), while vapor condensation releases sensible heat in the visible dry part of the sample ahead of the wetting front.

Fig 6. Diagram (left) showing relative locations where heat of wetting and vapor condensation occur.

Fig 7 shows the process in a high-permeability core (Boise sandstone); with infrared images to visualize temperature distribution across the core during the imbibition process.

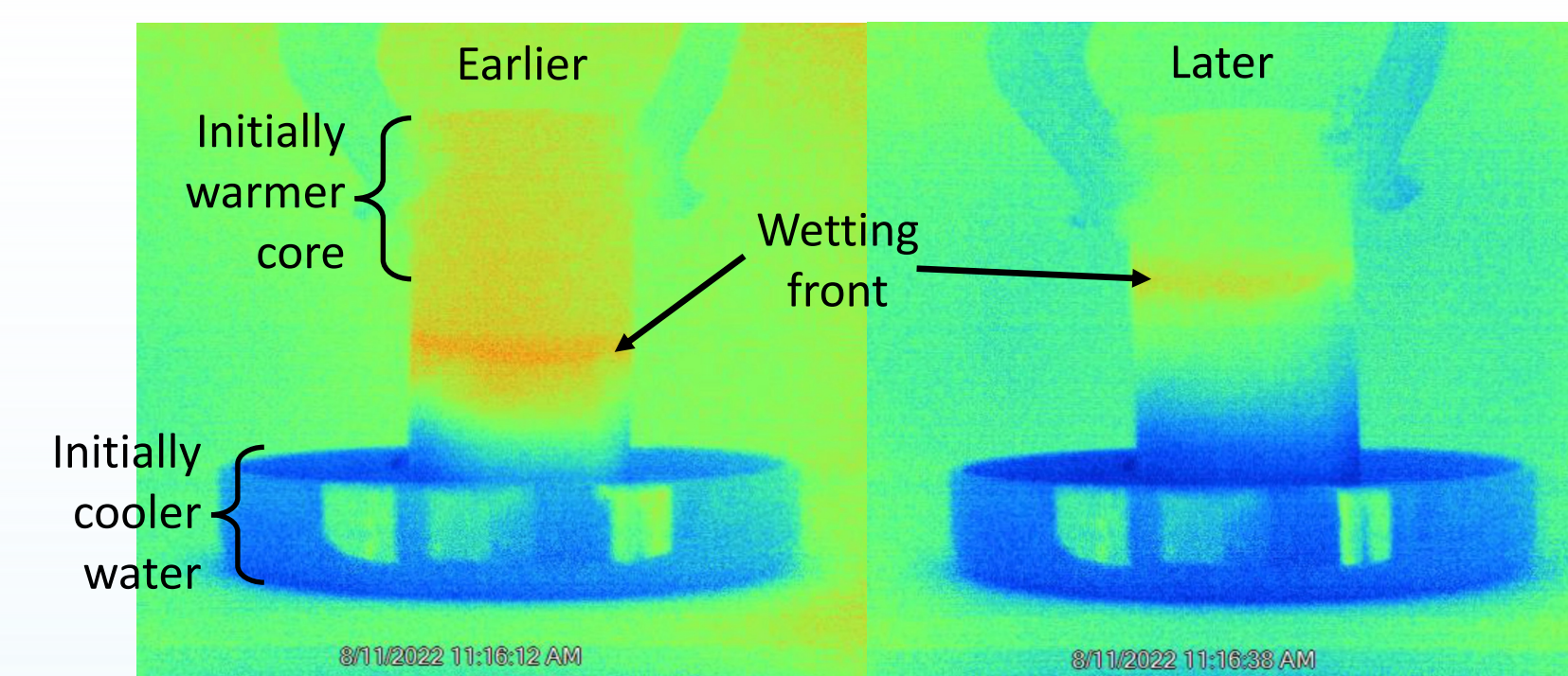


Fig 7. Infrared images during imbibition into Boise sandstone core (3 cm diameter). Warmest place at both times is at wetting front.

Cooler water imbibe into a room-temperature core. The water is slightly cooler due to evaporative effects. The infrared images clearly show the warmest place is the leading edge of the wetting front (warmer than the core or the water were initially). In this sample vapor migration ahead of the wetting front is minimal.

3. Vitric Tuff Results

For contrast against tests conducted in zeolitic tuff samples (Fig 1 & Fig 3), a vitric tuff sample was also tested. The wetting front took approximately 1 hour to imbibe to the top of the 17.5 cm long vitric tuff sample.

Fig 8 shows RTD and electrical resistance measurements acquired using a NI cDAQ. The RTD's were measured using 9219 and 9217 NI cModules, while electrical resistance measurements were measured using a Keithley 2604b source meter through a WireFlow 3132 multiplexer. The measured electrical resistance drops two orders of magnitude when the wetting front moves past an observation point. Photos were also used to estimate the wetting front elevation (Fig 9).

Vertical lines in Fig 8 at the resistance drop (top) and peak temperature (bottom), along with times and heights are plotted as points in Fig 10. The three types of data clearly are similar for this vitric core, where vapor migration ahead of the wetting front is minimal.

The slope of the line in Fig 10 is the sorptivity, S , (Philip, 1957), which has been related to the intrinsic permeability via regression methods (Tokunaga, 2020; equation to right). Here $\eta = 8.9 \times 10^{-4} \text{ [Pa} \cdot \text{s]}$ is viscosity, $\Delta\theta$ is the change in liquid saturation, and $j_2 = 0.0912 \text{ [Pa} \cdot \text{m}^{0.72}]$.

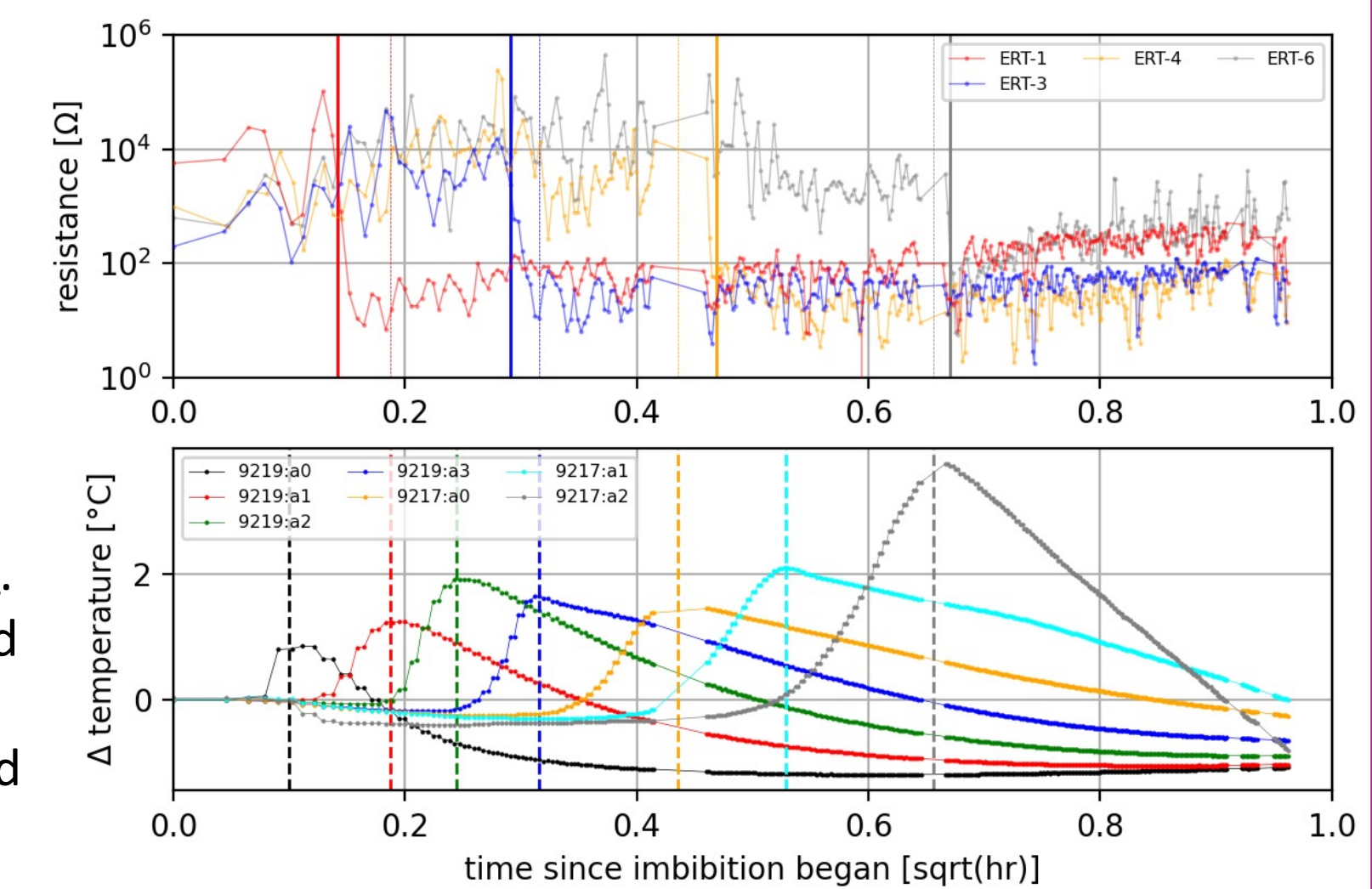


Fig 8. Temperature rise using RTDs (bottom) and resistance (top) vs. square root time for vitric tuff core

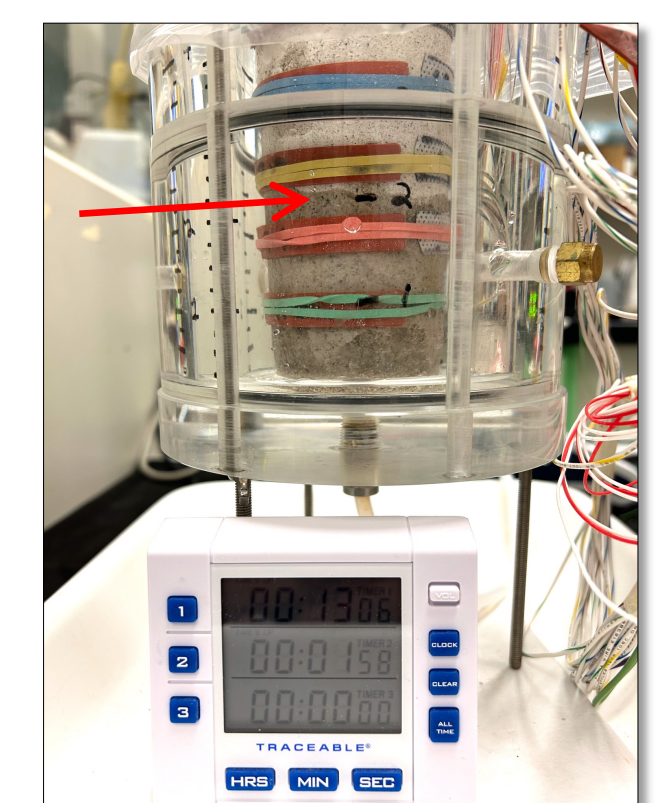


Fig 9. Photo of wetting front (red arrow) in vitric tuff core with RTD and resistance measurements.

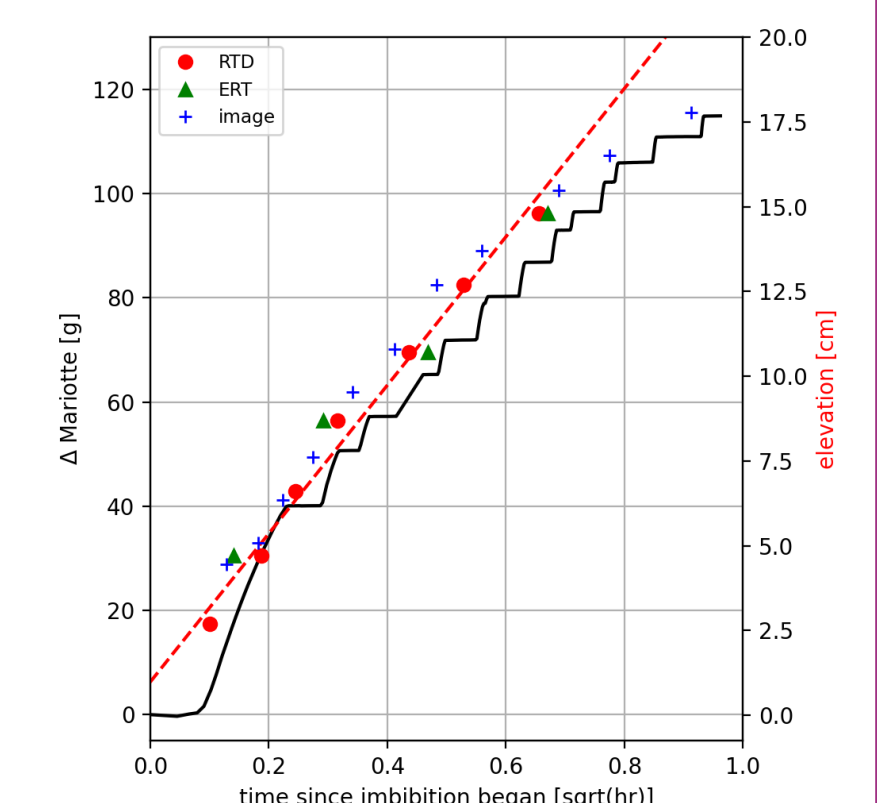


Fig 10. RTD (●), resistance (▲), and image (+) data showing wetting front progress. Line is $3.65 \times 10^{-3} \text{ m}/\sqrt{\text{s}}$ slope

The vitric tuff (Fig 10) has an estimated permeability of $3.1 \times 10^{-14} \text{ m}^2$, while the zeolitic tuff in (Fig 3) has an estimated permeability of $3.4 \times 10^{-16} \text{ m}^2$. These two samples illustrate the method applied to both high permeability (vitric) and low permeability (zeolitic) tuff samples.

4. Future Directions

Using RTDs and electrodes, data can be fit to an analytical solution (Good et al., 2023) or numerical models (Kuhlman et al., 2022b). This approach could be used to estimate flow (porosity, permeability), transport (tortuosity), and thermal (diffusivity) properties from one lab test.

References

Murali, V., Zeegers, J. C., & Darhuber, A. A. (2020). Infrared thermography of sorptive heating of thin porous media—Experiments and continuum simulations. *International Journal of Heat and Mass Transfer*, 147, 118875.
 Peters, R.R., E.A. Klavetter, J.T. George & J.H. Gauthier, 1987. "Measuring and modeling water imbibition into tuff" in Evans, D.D. & T.J. Nicholson (Eds.) *Flow and Transport Through Unsaturated Fractured Rock*, pp. 99-106. American Geophysical Union Monograph 42.
 Philip, J. R. (1957). The theory of infiltration: 4. Sorptivity and algebraic infiltration equations. *Soil science*, 64(3), 257-264.
 Tokunaga, T. K. (2020). Simplified Green-Ampt model, imbibition-based estimates of permeability, and implications for leak-off in hydraulic fracturing. *Water Resources Research*, 56(4), e2019WR026919.
 Żołądek-Nowak, J., Milczarek, J., Fijał-Kirejczyk, J., Żołądek, J., & Jurkowski, Z. (2012). Transient Thermal Phenomena during Spontaneous Water Migration in Zeolite Beds. *Acta Physica Polonica A*, 122(2), 415-418.
 Good, F. T., Kuhlman, K. L., LaForce, T. C., Paul, M. J., & Heath, J. E. (2023). Analytical solution and parameter estimation for heat of wetting and vapor adsorption during spontaneous imbibition in tuff. *International Journal of Heat and Mass Transfer*, 203, 123814.
 Heath, J.E. & K.L. Kuhlman, S.T. Broome, J.E. Wilson & B. Malama, 2021. Heterogeneous multiphase flow properties of volcanic rocks and implications for noble gas transport from underground nuclear explosions. *Vadose Zone Journal*, 20(3):e201213.
 Kuhlman, K.L., M.M. Mills, J.E. Heath & M.J. Paul, 2022a. *FY22 Progress on Multicontinuum Methods in Containment*. Sandia National Laboratories. doi:10.2172/1877460.
 Kuhlman, K.L., M.M. Mills, J.E. Heath, M.J. Paul, J.E. Wilson & J.E. Bower, 2022b. Parameter estimation from spontaneous imbibition into volcanic tuff. *Vadose Zone Journal*, 21(2):e20188.